Nanoscale

REVIEW

View Article Online
View Journal | View Issue

Check for updates

Cite this: *Nanoscale*, 2023, **15**, 3585

Improving the performance of quantum dot light-emitting diodes by tailoring QD emitters

Zhaohan Li,*†[a,b] Jiaojiao Song,†[b] Anming Li,[a] Huaibin Shen *[b] and Zuliang Du[b]

Received 16th December 2022,
Accepted 23rd January 2023

DOI: 10.1039/d2nr07078b

rsc.li/nanoscale

As the emitters of quantum dots (QDs) light-emitting diodes (QLEDs), QDs, which are responsible for the charge injection, charge transportation, and especially exciton recombination, play a significant role in QLEDs. With the crucial advances made in QDs, such as the advancement of synthetic methods and the understanding of luminescence mechanisms, QLEDs also demonstrate a dramatic improvement. Until now, efficiencies of 30.9%, 28.7% and 21.9% have been achieved in red, green and blue devices, respectively. However, in QLEDs, some issues are still to be solved, such as the imbalance of charge injection and exciton quenching processes (defect-assisted recombination, Auger recombination, energy transfer and exciton dissociation under a high electric field). In this review, we will provide an overview of recent advances in the study and understanding of the working mechanism of QLEDs and the exciton quenching mechanism of QDs in devices. Particular emphasis is placed on improving charge injection and suppressing exciton quenching. An in-depth understanding of this progress may help develop guidelines to direct QLED development.

1. Introduction

Quantum dots (QDs) are expected to be one of the most promising candidates for next generation displays in terms of their excellent optical characteristics, such as broad absorption spectra, tunable narrow emission spectra, and high photoluminescence (PL) quantum efficiency.[1–5] In 1994, the QDs were first used in electroluminescent (EL) devices as light emitters.[6] Then, after about three decades of development, the performances of QD based light emitting devices (QLEDs) have been greatly improved by virtue of the improvement of QD synthesis, device structure engineering, and the in-depth understanding of the luminescence mechanism of QDs and the working mechanism of QLEDs.[7–14] Until now, the external quantum efficiencies (EQE) of 30.9%,[15] 28.7%[16] and 21.9%[16] have been achieved in red, green and blue devices, respectively.

As the emission centers of QLEDs, QDs play a crucial role in the efficiency, luminance and lifetime of devices. Also, with the important advances made in QDs, such as the deep understanding of ligand engineering and structure engineering,[1,3,17] the performances of QLEDs have also been dramatically improved. Therefore, insights from these progresses will be helpful to develop a set of guidelines to direct QLED innovation. In this review, we will provide an overview on recent advances in the understanding of the working mechanism of QLED devices and the approaches to improve device performances.

2. The working mechanism of QLEDs

Since the first report of electrically driven QLEDs in 1994, four device structure types, which are QLEDs with a single-layer polymer, all-organic, all-inorganic, and organic–inorganic hybrid charge transport layer (CTL), have evolved nearly chronologically. With the evolution of the device structure and in-depth understanding of the working mechanism of QLEDs, the device performances have been greatly improved. Summaries of recent advances in QLEDs are shown in Table 1.

At present, the organic–inorganic hybrid structure is the most commonly used device structure. Also, most of the high-performance devices are based on the conventional organic–inorganic hybrid structure.[15,18,23,29,35] Generally, the QLEDs with the conventional structure have 4 functional layers, as shown in Fig. 1, that is, a hole injection layer (HIL), hole transport layer (HTL), QD emitting layer (EML) and electron transport layer (ETL). Under the driving of an external electric field,

[a]*College of Physics and Electrical Engineering, Zhengzhou Normal University, Zhengzhou 450044, China. E-mail: lizhaohan22@163.com*
[b]*Key Laboratory for Special Functional Materials of Ministry of Education, National & Local Joint Engineering Research Center for High-Efficiency Display and Lighting Technology, Henan University, Kaifeng 475004, China. E-mail: shenhuaibin@henu.edu.cn*
† These authors contributed equally to this work.

Table 1 Summaries of recent advances in QLEDs

Colors	Year	Device structure	EL (nm)	EQE_{max} (%)	L_{max} (cd m^{-2})	V_{on} (V)	Lifetime	Ref.
Red	2014	ITO/PEDOT:PSS/poly-TPD/PVK/QDs/PMMA/ZnO/Ag	640	20.5	42 000	1.7	L_0 = 100 cd m^{-2}, T_{50} > 100 000 h	7
	2015	ITO/PEDOT:PSS/TFB/QDs/ZnO/Al	625	12.0	21 000	1.5	L_0 = 100 cd m^{-2}, T_{50} > 300 000 h	18
	2018	ITO/PEDOT:PSS/TFB/QDs/ZnO/Al	631	15.1	—	1.7	L_0 = 100 cd m^{-2}, T_{50} > 2 200 000 h, L_0 = 1000 cd m^{-2}, T_{95} > 2300 h	19
	2018	ITO/PEDOT:PSS/poly-TPD/PVK/QDs/ZnMgO/Ag	624	18.2	—	1.7	L_0 = 100 cd m^{-2}, T_{50} = 190 000 h	20
	2018	ITO/ZnO + PVP/QDs/TCTA/MoO_x/Al	~611	13.5	—	1.9	L_0 = 100 cd m^{-2}, T_{50} = 1 330 000 h, L_0 = 1000 cd m^{-2}, T_{50} = 23 660 h	21
	2019	ITO/NiO_x–BA–CF_3/poly-TPD/QDs/ZnMgO/Ag	625	13.4	—	1.65	L_0 = 1000 cd m^{-2}, T_{95} = 2500 h	22
	2019	ITO/PEDOT:PSS/TFB/QDs/ZnO/Al	601	21.6	357 000	~1.92	L_0 = 100 cd m^{-2}, T_{50} > 1 600 000 h, L_0 = 7000 cd m^{-2}, T_{50} > 840 h	23
	2019	ITO/PEDOT:PSS/TFB/QDs/ZnO/Al	602	30.9	334 000	1.9	L_0 = 100 cd m^{-2}, T_{50} > 1 800 000 h, L_0 = 2000 cd m^{-2}, T_{50} > 7300 h	15
	2020	ITO/PEDOT:PSS/TFB/QDs/ZLMO@MO/Al	636	20.6	—	1.7	L_0 = 1000 cd m^{-2}, T_{95} > 11 000 h	24
	2020	ITO/PEDOT:PSS/poly-TPD/PVK/QDs/ZnMgO/Ag	—	20.2	—	1.65	L_0 = 1000 cd m^{-2}, T_{95} = 3800 h	25
	2020	ITO/ZnO/QDs/CBP:BCBP/MoO_x/C_{60}/Al	~610	18.3	410 000	~2.56	L_0 = 100 cd m^{-2}, T_{70} = 2 140 000 h	26
	2021	Ag/ZnO/QD/CBP/MoO_x/HAT–CN–Ag	615	14.7	650 000	—	L_0 = 100 cd m^{-2}, T_{50} = 12 600 000 h	27
	2022	ITO/PEDOT:PSS/TFB/QDs/ZnO/Al	~624	21.9	—	1.7	L_0 = 1000 cd m^{-2}, T_{95} > 21 000 h	28
Green	2015	ITO/PEDOT:PSS/TFB/QDs/ZnO/Al	537	14.5	—	2.0	L_0 = 100 cd m^{-2}, T_{50} > 90 000 h	18
	2017	ITO/PEDOT:PSS/TFB/QDs/ZnO/Al	532	16.5	78 000	2.2	L_0 = 100 cd m^{-2}, T_{50} > 480 000 h	29
	2018	ITO/ZnO/PVK/QD/PEIE/poly-TPD/MoO_x/Al	525	22.4	72 814	5.75	—	30
	2019	ITO/PEDOT:PSS/TFB/QDs/ZnO/Al	~534	22.9	614 000	—	L_0 = 100 cd m^{-2}, T_{50} > 1 760 000 h, L_0 = 7000 cd m^{-2}, T_{50} > 770 h	23
	2020	ITO/PEDOT:PSS/TFB/QDs/ZnO/Al	530	23.9	~13 200	~2.2	L_0 = 100 cd m^{-2}, T_{50} > 1 655 000 h, L_0 = 1000 cd m^{-2}, T_{95} > 2500 h	31
	2022	ITO/PEDOT:PSS/PF8Cz/QDs/ZnMgO/Al	537	28.7	—	2.05	L_0 = 100 cd m^{-2}, T_{95} ~ 580 000 h, T_{50} ~ 2 570 000 h	16
Blue	2015	ITO/PEDOT:PSS/PVK/QDs/ZnO/Al	455	10.7	4000	2.6	—	18
	2017	ITO/PEDOT:PSS/PVK/QDs/ZnO/Al	468	19.8	4890	5.1	L_0 = 100 cd m^{-2}, T_{50} = 47.4 h	32
	2019	ITO/PEDOT:PSS/TFB/QDs/ZnO/Al	~481	8.05	62 600	—	L_0 = 100 cd m^{-2}, T_{50} > 7000 h, L_0 = 7000 cd m^{-2}, T_{50} > 6 h	23
	2020	ITO/PEDOT:PSS/TFB/QDs/ZnMgO/Al	460	20.2	88 900	—	L_0 = 100 cd m^{-2}, T_{50} = 15 850 h	33
	2022	ITO/PEDOT:PSS/PF8Cz/QDs/ZnMgO/Al	479	21.9	—	2.45	L_0 = 100 cd m^{-2}, T_{95} ~ 4400 h, T_{50} ~ 24 000 h	34

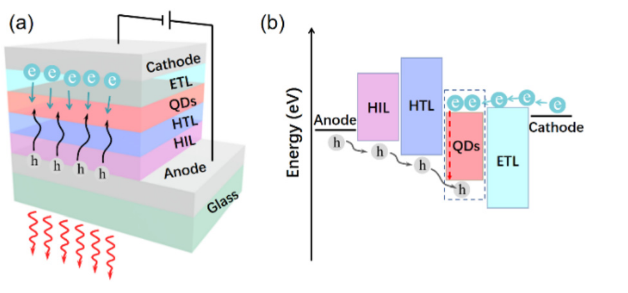

Fig. 1 (a) Schematic illustration of QLEDs with the traditional structure. (b) Energy band diagram of QLEDs and the schematic illustration of charge injection and charge recombination in QLEDs.

the holes are injected into the HIL from the anode of QLEDs. Then, the holes go through the HTL and are injected into the EML. Similarly, the electrons go through the ETL and are injected into the EML. If the electrons and holes in the QDs recombine radiatively, the QLEDs will give out light.

For QLEDs, EQE, which is an important performance parameter, is equal to the ratio between the number of photons emitted from the device and the number of carriers injected into the device.[36,37] Generally, EQE depends on three factors: the fraction of carriers effectively injected into QDs, the fraction of excitons that deexcite radiatively, and the fraction of photons that effectively eject from devices. And it can be expressed by the following equation:[38]

$$\eta_{EQE} = \gamma \times \eta_r \times \eta_{out}$$

where γ is the ratio of carriers injected into QDs that form excitons, η_r is the fraction of excitons in QDs that recombine radiatively under operational conditions and η_{out} is the light outcoupling efficiency.[38] γ is associated with the fraction of carriers injected into QDs, and the ratio of injected holes to electrons. While, in QLEDs the electron injection barrier is much lower than the hole injection barrier; therefore, the electrons are injected more efficiently than holes. η_r is associated with the fraction of excitons recombined radiatively, and it relates to the quenching mechanisms of working QLEDs, such as defect-assisted recombination, Auger recombination, energy transfer and electric field quenching under high electric field. Carrier injection efficiency and quenching mechanisms are two important issues associated with device efficiency. In this regard, the design criteria of QD emitters for improving QLED performance are high charge injection and high radiative recombination efficiency. As for charge injection, it needs the coordination between the QD layer and other functional layers. The factors influencing radiative recombination include the trapping of carriers by defects, the nonradiative quenching processes and electric field induced quenching. In this review, we will mainly discuss the ways of improving charge injection and radiative recombination from the QD aspect, and discuss the methods to improve QLED performance in three sections: carrier injection efficiency, defects and quenching processes.

3. Improving carrier injection efficiency to enhance the performance of QLEDs

In QLED devices, the band offset between the Fermi energy level of the anode and the valence band maximum (VBM) of QDs is generally much larger than that between the Fermi energy level of the cathode and the conduction band of QDs, especially for the blue light-emitting devices.[39] Therefore, in QLEDs, the electron injection efficiency far outpaces hole injection efficiency. And this is the main reason why the blue devices are far beneath their green or red counterparts in efficiency, luminance and device lifetime. Until now, many research groups have demonstrated that the performance of devices was improved by balancing charge injection. In this regard, as for the QD emitters, it is better to employ the QDs with high VBM to fabricate QLEDs.[15,18,19,23] The electronic properties of QDs are dependent on the QD size, chemical composition and the surface ligand of QDs. Therefore, by tailoring the nanostructure and ligand of QDs, the hole injection is expected to be improved, and then the charge injection could be balanced.

3.1. Tailoring the ligands of QDs to improve charge injection

Because of high surface-to-volume ratio, the surfaces of QDs are generally coordinated with the organic ligands to stabilize QDs. The electrical conductivity and energy level of QDs can be tuned by tailoring QD ligands. Therefore, in devices, the surface ligands of QDs play a significant role in charge transport. And much progress in QLEDs was made by tailoring QD ligands.

It is known that most organic ligands act as bulky insulating barriers between QDs, hindering charge transport.[40] The poor conductivity of emitting layers, which is highly related to the long-chain organic ligand, constrains the luminance and efficiency of QLEDs. In 2015, Shen *et al.* reported that the electron mobility and hole mobility of the QD film all increased by

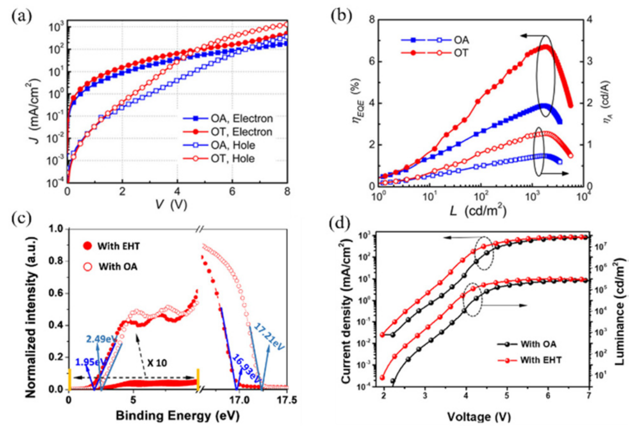

Fig. 2 (a) Current density–voltage (J–V) characteristics of electron- and hole-only devices based on OA capped QDs and OT capped QDs; (b) EQE and current efficiency of the devices based on QDs with OA and OT ligands as a function of luminance (L). Reproduced with permission.[41] Copyright 2015, American Chemical Society. (c) Ultraviolet photoelectron spectroscopy data of $Zn_{1-x}Cd_xSe/ZnSe/ZnS$ core/shell QDs with OA or EHT surface ligands; (d) current density and luminance *versus* bias for devices based on $Zn_{1-x}Cd_xSe/ZnSe/ZnS$ core/shell QDs with OA or EHT surface ligands. Reproduced with permission.[15] Copyright 2019, WILEY-VCH.

replacing the longer oleic acid (OA) ligand with shorter 1-octanethiol (OT) ligand, as shown in Fig. 2(a). More importantly, the ligand exchange promoted the charge balance of QLEDs, and the blue devices showed an unprecedented high EQE of 12.2%, as shown in Fig. 2(b).[41] By exchanging the intrinsic ligand OA with a short chain ligand tris(mercaptomethyl) nonane (TMMN), the QLEDs based on QDs capped with TMMN showed much higher efficiency and luminance and much lower turn-on voltage than the devices based on QDs coordinated by OA.[29] Small inorganic ligands are also advantageous for charge injection/transport in QD based devices. In 2018, the Sargent group implemented conductive halides in Zn chalcogenide-shelled QDs to improve carrier mobility. The resulting devices demonstrated a reduced turn-on voltage of 2.5 V and maximum luminance of 460 000 cd m^{-2}, which was the highest value reported thus far.[42] In 2020, Kim *et al.* exchanged the native OA ligand of ZnTeSe/ZnSe/ZnS core/shell/shell (C/S/S) QDs with $ZnCl_2$ through two steps of ligand exchange: a liquid-phase treatment (referred to as C/S/S–Cl(l)) and a film-washing treatment (referred to as C/S/S–Cl(f)). And they fabricated a QLED with a double EML consisting of C/S/S–Cl(l) and C/S/S–Cl(f) layers to improve charge injection/transport and recombination simultaneously. The resulting device showed an EQE of 20.2% and T_{50} lifetime of 15 850 h at 100 cd m^{-2}, which were the highest values reported thus far for blue QLEDs.[33]

Surface ligands not only influence the conductivity between QDs, but also the electronic properties. Upon ligand coordination, generally, the energy level of QDs will shift to a higher or lower energy direction. The shifts of energy levels originate from the induced dipole at the ligand/QD interface and the intrinsic dipole of the ligand.[43,44] Ligand-induced energy level shifts are proved to be an important means to control the electronic properties of QDs and to optimize the performance of QD based optoelectronic devices. By engineering the band alignment of the QDs through ligand treatments, the QD solar cell showed a certified efficiency of 8.55% in 2014.[45] Much work in the QLED field has also demonstrated that the ligand treatments are of great benefit to energy level tuning and charge balance. By exchanging the native OA ligand with tris (mercaptomethyl)nonane (TMMN), the VBM of TMMN-capped QDs shifts to the higher energy direction; moreover, the charge injection and charge balance are greatly improved for the corresponding QLED devices.[29] Similarly, by exchanging the ligand OA with 2-ethylhexane-1-thiol (EHT), as shown in Fig. 2(c), the VBM of EHT-capped QDs is 0.27 eV higher than that of OA-capped QDs. Consequently, the QLEDs based on EHT-capped QDs showed much better charge injection and higher EQE than the devices based on QDs capped with native OA ligand, as shown in Fig. 2(d).[15]

3.2. Tailoring the nanostructure of QDs to improve the charge injection

The electronic properties of QDs are dependent on both the surface chemistry and the nanostructure including the composition and the thickness of the core and shell. In recent years, many researchers have engaged in tailoring the nanostructure of QDs to improve charge injection. It is known that the injection efficiency of electrons is much lower than that of holes, especially for green and blue QLEDs. Therefore, in order to enhance the hole injection efficiency of green/blue devices, high VBM and relatively wide bandgap are simultaneously required for the emitters. However, generally, the inorganic materials with high VBM have a relatively narrow bandgap. As shown in Fig. 3, ZnSe not only has a relatively higher VBM, but also a wide enough bandgap to confine electron and hole wavefunctions. In this regard, maybe ZnSe is one of the most suitable inorganic semiconductors to serve as the shell of QDs.

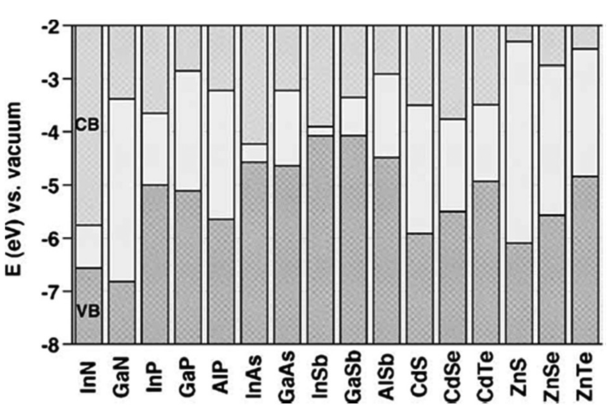

Fig. 3 Electronic energy levels of selected III–V and II–VI semiconductors using the valence-band offsets. Reproduced with permission.[46] Copyright 2009, Wiley-VCH.

Recently, many advances were made in QLEDs by employing ZnSe based QDs. In 2015, the Qian group[18] reported a full series of blue, green and red QLEDs with the efficiencies all over 10% by elaborately tailoring the nanostructure of QDs. They synthesized two kinds of QDs with ZnSe-rich and CdS-rich intermediate shells, respectively. As the VBM of ZnSe is 0.2 eV higher than that of CdS, the hole injection barrier is reduced with a ZnSe-rich intermediate shell, leading to a much higher injection current density ($V > 3$ V) than the CdS-rich QD based device. Consequently, the green devices based on ZnSe-rich QDs exhibited a much higher EQE than CdS-rich QD based devices. Following this energy design strategy, in 2018 the Qian group[19] further synthesized CdSe/$Cd_{1-x}Zn_xSe$/ZnSe QDs (ZnSe-QDs) with a high VBM ZnSe shell, which favors efficient hole injection. In terms of the higher VBM of ZnSe-QDs, the valence band offset at the TFB/ZnSe-QD interface is much smaller than that at the TFB/ZnS-QD interface. This excellent alignment of the VBM and HOMO between ZnSe-QDs and TFB interface is helpful for significantly declining the hole injection barrier in the corresponding QLEDs. Finally, the devices based on these tailored ZnSe-QDs exhibited much extended operation lifetime (T_{50} > 2 200 000 h@100 cd m^{-2}). The device lifetime is the key performance parameter for the commercialization of QLEDs. The device lifetime of QLEDs is usually characterized by T_{50} (or T_{95}), defined as the time for the luminance to decrease to half (or 95%) of its initial luminance while operating at a constant current density. The instability of devices is mainly induced by the imbalanced charge injection. Chang *et al.*[47] pointed out that the leaking of excessive electrons into the HTL would lead to irreversible degradation of devices and reduces device lifetime. In 2019, Chen *et al.*[48] demonstrated that differing from red QLEDs, the poor lifetime of blue QLEDs originates from the fast degradation at the QD–ETL junction. Therefore, improvement of charge injection and the balance of charge injection are also favourable for device stability.

In 2019, our group also employed QDs with high VBM to fabricate QLEDs. And these red, green and blue CdSe/ZnSe QD based QLEDs demonstrate simultaneously high brightness and EQE (21.6%@13 300 cd m^{-2}, 22.9%@52 500 cd m^{-2}, and 8.05%@10 100 cd m^{-2} for red, green and blue devices, respectively). The high performance of devices can mainly be attributed to the Se throughout the whole of QDs, which could reduce the hole injection barrier, enhance the charge balance effectively, and consequently improve the device performance.[23]

The devices with high performance are the result of the coordination of all the functional layers. Therefore, besides tailoring QDs to improve charge injection, optimization of other functional layers, such as tuning the CTL, cathode and adding an additional blocking layer,[7,49–53] could also enhance the device performances. In 2014, the Peng group[7] improved the balance of charge injection by inserting a PMMA insulating layer, and the resulting devices demonstrated a record-high efficiency of 20.5%. In 2019, the Tan group[53] demonstrated that the charge injection could be balanced through the CTL doping strategy and the device lifetime was improved ~3.5 times.

Relatively, designing new charge transporting materials or adding additional layers significantly increases the technical difficulty and cost of commercial production. Therefore, it is believed that QD structure design is the most direct, effective, convenient and low-cost method to improve device performance, and also is the most promising method to improve device performance.

4. Reducing the defects to enhance the performance of QLEDs

Due to the large surface-to-volume ratio, there may exist a great many defects in the interface of QDs and the surface of QDs. The defects in QDs, especially the midgap defects, may form carrier traps to capture the electrons or holes, as shown in Fig. 4(a). Since a great number of carriers will be trapped by the defect states and therefore immobile, only part of the carriers injected into the QDs can be considered as free charges.[54] Therefore, the defects in QDs will inevitably lead to the lowered current density and the inefficiency of devices.

Until now, great efforts have been adopted to reduce the defects of QDs, such as surface engineering and interfacial engineering. In 2016, the Peng group[55] employed two ways—shell isolation and surface treatment—to battle the surface traps. They demonstrated that the electron traps of CdSe/CdS core/shell QDs could be readily isolated from the electron wavefunction of the excitons with more than ~2 monolayers of the CdS shell. In general, the shell with a wide bandgap could isolate the surface traps from the wavefunction of excitons. According to this design strategy, the Peng group[9] synthesized $Cd_xZn_{1-x}Se$/ZnSe/ZnS core/shell QDs through two complementary steps by localizing exciton wavefunctions away from the inorganic–organic interface of QDs. They first synthesized uniform-alloy $Cd_xZn_{1-x}Se$ QDs with their physical size greater than the exciton diameter to confine the excitons away from the inorganic–organic interface. Subsequently, by epitaxially growing wide bandgap and high-quality shells, the interface effects on the excitons can be reduced to a negligible level. The as-synthesized QDs exhibited a record-low PL full width at half-maximum (16.3 for ensemble PL and 9.7 nm for single-dot PL).

Due to the lattice mismatch of the core and shell in QDs, the core/shell QDs usually endure many interfacial defects. As interfacial defect states are more accessible than surface defects for the excitons, generally, the interfacial defects play a much more important role in the photoelectric properties of QDs and devices. Due to the gradual change of lattice constants, the alloyed QDs will have relatively fewer interfacial defects. By applying complementary analytical techniques of electron microscopy and atom probe tomography, Chae *et al.* elucidated the internal structure and related atomic distribution of core/shell structured CdSSe/ZnS QDs in three dimensions, particularly at heterostructure interfaces. The $Cd_xZn_{1-x}S$ gradient inner shell between the CdSe core and ZnS outermost shell alleviates the lattice misfit strain at the interfaces, thereby enhancing PL QY and photostability to a greater extent than those of other single-shell structures.[56]

In one aspect, the defects in QDs will decrease the quantity of free carriers; in the other aspect, the trapped carriers will lead to the charging of QDs and the enhancement of non-radiative Auger recombination, which will be further discussed in section 5.1.

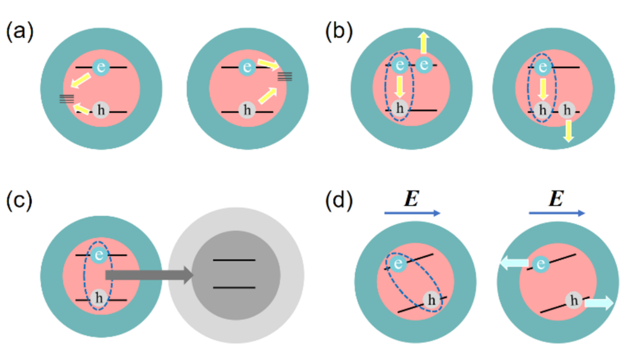

Fig. 4 Schematic illustration of exciton quenching processes. (a) Trap-assisted recombination; (b) Auger recombination; (c) energy transfer to non-emissive QDs; (d) field-induced reduction in the overlap between electron and hole wavefunctions and field-induced exciton disassociation.

5. Suppressing the exciton quenching processes to enhance the performance of QLEDs

The exciton dynamics is determined by the interactions with their surroundings, including scattering with the defects, free carriers, other excitons, phonons, *etc.*[57] The carriers injected into QDs may recombine *via* the radiative process or non-radiative process. Generally, the radiative lifetime of excitons in QDs is on a time scale of tens of nanoseconds (ns). In this period, the excitons may interact with defects and be captured by the trap states, or interact with other excitons and free carriers, and then deexcite *via* the Auger process.

5.1. Suppressing Auger recombination

The Auger recombination is a three-particle nonradiative recombination process. In this process, the energy released by the recombined exciton will be absorbed by the other carrier (an electron or a hole), as shown in Fig. 4(b). Auger recombination dominates the dynamical behavior of multicarrier states in QDs. Unfortunately, QDs in the working QLEDs are generally in multicarrier states. As mentioned above, the defects may lead to the charging of QDs and eventually lead to the enhancement of the Auger process. Moreover, in terms of the disparity of carrier injection efficiency, the QDs in QLEDs are commonly negatively charged. The charged QDs will readily undergo the Auger process. More importantly, at high current density, there is commonly more than one exciton in a QD. Due to the much higher rates of the Auger process than the radiative process, the QDs in multi-exciton states will deexcite easily *via* the nonradiative Auger process. In QLEDs, suppressing Auger recombination is expected to enhance the device performance. And many advances have been made in the suppression of Auger recombination. It is found that Auger recombination is more efficient in the QDs with abrupt confinement potential than QDs with soft confinement potential.[58] Smoothing of the confinement potential can be achieved by forming an alloyed interface at the core/shell. The Yang group[59] synthesized CdZnS/ZnS core/shell QDs with a thicker shell and more smooth core/shell interface through prolonging the high-temperature shelling duration. It is demonstrated that the efficiency of 3 h shelled QD based devices is much higher than that of 1 h shelled QD based devices. In 2014, the Klimov group[60] demonstrated that the $CdSe_xS_{1-x}$ interfacial alloy layer could enhance the biexciton emission efficiency, while having essentially no effect on single-exciton decay.

5.2. Suppressing the energy transfer process

The exciton in one QD may deexcite to the ground state by transferring its energy to the adjacent QD, and then excite an exciton in the adjacent QD. The energy transfer processes, which are highly related to the spacing between the two excitons that undergo energy transfer,[61] are more active in closely packed QD films than in the QD solution. Energy transfer processes will lead to a significant reduction in solid-state PL QYs due to exciton diffusion and transfer to non-emissive QDs possessing trap sites, as shown in Fig. 4(c).

As the QDs in QLEDs are in the form of densely packed films, the performances of QLEDs are to a large extent restricted by the energy transfer processes. In 2012, Pal *et al.*[62] synthesized CdSe/CdS core/shell QDs with different shell thicknesses to study the influence of shell thickness on device performance. They assessed the effect of increasing shell thickness on the energy transfer process through time-resolved PL spectra of QD solution and QD solid films. As shown in Fig. 5, with the increase of shell thickness, the PL lifetime of CdSe/CdS QDs increases monotonically. Moreover, the PL dynamics of thin-shell CdSe/CdS QDs measured at shorter excitation wavelength becomes significantly faster when passing from diluted solution to solid film. This is a signature of energy transfer process from QDs with a wider bandgap to QDs with a narrower bandgap. With the increase of shell thickness, the discrepancy between QD solution and QD film PL dynamics is progressively reduced. As shown in Fig. 5(d), for the CdSe/16CdS core/shell QD film, the spectral diffusion is completely suppressed. It is because the thick shell could act as a spacer between the interacting excitons in the neighboring CdSe/CdS core/shell QDs, suppressing distance-dependent interparticle interactions.

Many groups have reported that the thick shell of QDs could effectively suppress the energy transfer process. The experiment results demonstrated that the PL spectra of the

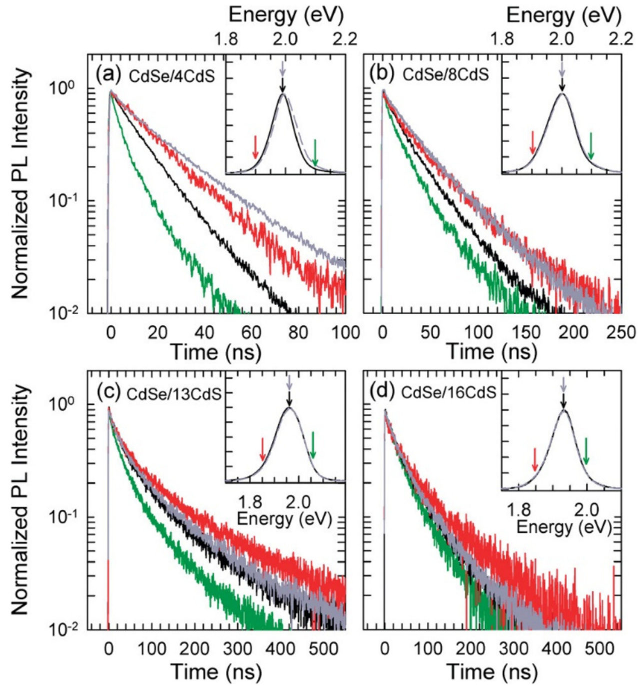

Fig. 5 PL decay curves of CdSe/CdS QD solution (gray lines) and film (red, black and green lines) with a (a) 4, (b) 8, (c) 13, and (d) 16 monolayer CdS shell. Inset: The PL spectrums of CdSe/CdS QD solution (solid black curves) and film (dashed gray curves). The PL decay curves are collected at the emission energies indicated by the arrows in the insets. Reproduced with permission.[62] Copyright 2012, American Chemical Society.

ZnCdSe/ZnS QD solid film shift to the longer wavelength side in comparison with that of the QD solution. Moreover, with increasing the shell thickness, the extent of redshift decreases gradually. This also indicates that the thick shell could suppress the energy transfer process of the close-packed film.[63] Similarly, Yang *et al.* reported that by increasing shell thickness, the ZnSe/ZnS/ZnS QD-based devices exhibited suppressed Förster resonance energy transfer (FRET) compared with ZnSe/ZnS QD-based devices.[34]

5.3. Electric-field induced quenching

The electron–hole pair in QDs will be separated in opposite directions by the external electric field. As shown in Fig. 4(d), the reduction in the overlap of electron and hole wavefunctions in consequence of the field-induced charge delocalization will lower the radiative recombination rate, and quench the QD PL. In 2013, Bozyigit *et al.* employed a QD capacitive structure to investigate the effect of electric field on the PL decay and PL QY of the QD film. The results demonstrated that high electric fields (0.5–4 MV cm^{-1}) showed a strong quenching effect on PL QY but had little effect on the PL lifetimes. Therefore, they deduced that the reduced QYs at high electric field could be attributed to the field-induced spatial separation of electron and hole wavefunctions, rather than nonradiative processes.[64] Unfortunately, in the working

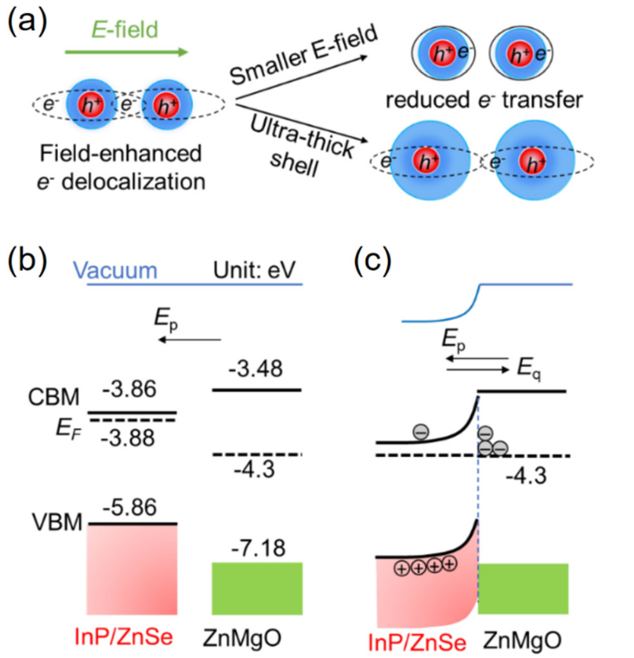

Fig. 6 (a) Schematic illustration of the field-enhanced electron delocalization and the two feasible ways to alleviate its impacts on charge transfer. The energy level alignments of the InP/ZnSe layer and ZnMgO (b) when they are separated, and (c) when they are in close contact. Reproduced with permission.[65] Copyright 2022, Wiley-VCH.

QLEDs, the electric field across QDs generally is about 10^8 V m^{-1} to materials with a high mobility of 10^{-2} m^2 V^{-1} s^{-1}.[54] The high electric field generally will inevitably lead to the inefficiency of QLEDs.

Meanwhile, the field-induced charge delocalization will lead to the enhancement of energy transfer, due to the decrease of spacing between the interacting excitons. Therefore, as shown in Fig. 6(a), the field-induced energy transfer can be suppressed by increasing the shell thickness or reducing the electric field across QDs.[65] Moreover, at high enough electric fields, the coulombic binding of excitons can be overcome, resulting in dissociation and formation of free carriers.[66,67] Xie *et al.* applied a reverse-biased QLED to study the electric field effect on QD PL. And they pointed out that the 99.5% reduction in PL was accomplished by a synergistic interplay of the quantum-confined Stark effect and field-induced exciton dissociation.[66] The electric field across QDs is determined by the external electric field and the built-in field, which is induced by the accumulated charges at the interface of the QD layer and charge transport layer.[65,68] The mismatched Fermi levels induced a diffusion potential (V_{diff}), which will drive the electron transfer from QDs into the EML. As shown in Fig. 6(b), a pseudo-electric-field $E_p = V_{diff}/d$ is used to quantify the driving force of the electron diffusion. When the QD film and ZnMgO layer are in contact, as shown in Fig. 6(c), the electrons will accumulate at the ZnMgO side and holes at the QD side to make the Fermi levels aligned with each other. The accumulated charges can induce a built-in field (E_q), which will cancel out E_p. Therefore, the built-in field can partially cancel out the small applied bias. By reducing the effective electric field (at 2 V bias), a record-high EQE of 22.56% and luminance of 136 090 cd m^{-2} were achieved in InP-based QLEDs by Li *et al.*[65]

6. Summaries and perspectives

Through more than two decades of development, numerous advances have been made in QLEDs. And now, the performances of QLEDs could be comparable to that of the state-of-the-art OLEDs. Two main factors limiting the performance of QLEDs are charge injection efficiency, which is mainly induced by the potential barriers for electrons and holes, and radiative recombination efficiency, which is affected by various exciton quenching processes. In this review, we firstly present an overview on recent advances in the study and understanding of the working mechanism of QLEDs and the exciton quenching mechanism of QDs in devices. An in-depth understanding of the working mechanism is helpful to develop a set of guidelines to direct QLED innovation. As for QDs, the key criterion for ensuring high performance QLEDs is high charge injection efficiency and radiative recombination efficiency. Then, we mainly summarize the approaches to improve device performance from the QD aspect, such as improving charge injection, reducing defects of QDs, and suppressing various exciton quenching processes.

From the results of recent advances in QLEDs, it is believed that the following aspects will be critical to enhance the device performance.

6.1. Thick-shell QDs

The thick shell of QDs could not only effectively confine the exciton wavefunction to reduce the impact of surface trap states, but also act as a spacer to suppress energy transfer processes. Moreover, thick-shell QDs can also suppress field-induced quenching due to the dielectric shielding effect of the thick-shell.

6.2. Gradient alloyed QDs

In terms of the gradual change of lattice constant, the alloyed QDs will have fewer interfacial defects. More importantly, the soft-confinement potential will be beneficial to suppress Auger recombination which is very active in quantum-confined systems. However, meanwhile the alloyed QDs may suffer from decreased radiative recombination especially at high electric field due to the weaker confinement of exciton wavefunctions.

6.3. QDs with high VBM

The QDs with high VBM could improve hole injection efficiency and balance charge injection, leading to the enhancement of device performance.

Conflicts of interest

There are no conflicts to declare.

Acknowledgements

The authors gratefully acknowledge the research project of the National Natural Science Foundation of China (No. 61904161, U22A2072, 61905094, 61874039, 61922028, 62234006).

References

1 O. Chen, J. Zhao, V. P. Chauhan, J. Cui, C. Wong, D. K. Harris, H. Wei, H.-S. Han, D. Fukumura, R. K. Jain and M. G. Bawendi, *Nat. Mater.*, 2013, **12**, 445–451.
2 C. Pu, H. Qin, Y. Gao, J. Zhou, P. Wang and X. Peng, *J. Am. Chem. Soc.*, 2017, **139**, 3302–3311.
3 K. Boldt, N. Kirkwood, G. A. Beane and P. Mulvaney, *Chem. Mater.*, 2013, **25**, 4731–4738.
4 Y. Shirasaki, G. J. Supran, M. G. Bawendi and V. Bulović, *Nat. Photonics*, 2013, **7**, 13–23.
5 T. Meng, Y. Zheng, D. Zhao, H. Hu, Y. Zhu, Z. Xu, S. Ju, J. Jing, X. Chen, H. Gao, K. Yang, T. Guo, F. Li, J. Fan and L. Qian, *Nat. Photonics*, 2022, **16**, 297–303.
6 V. L. Colvin, M. C. Schlamp and A. P. Alivisatos, *Nature*, 1994, **370**, 354–357.
7 X. Dai, Z. Zhang, Y. Jin, Y. Niu, H. Cao, X. Liang, L. Chen, J. Wang and X. Peng, *Nature*, 2014, **515**, 96–99.
8 Y. Chen, J. Vela, H. Htoon, J. L. Casson, D. J. Werder, D. A. Bussian, V. I. Klimov and J. A. Hollingsworth, *J. Am. Chem. Soc.*, 2008, **130**, 5026–5027.
9 L. Huang, Z. Ye, L. Yang, J. Li, H. Qin and X. Peng, *Chem. Mater.*, 2021, **33**, 1799–1810.
10 D. H. Son, S. M. Hughes, Y. Yin and A. Paul Alivisatos, *Science*, 2004, **306**, 1009–1012.
11 P. O. Anikeeva, J. E. Halpert, M. G. Bawendi and V. Bulović, *Nano Lett.*, 2009, **9**, 2532–2536.
12 D. Bozyigit and V. Wood, *MRS Bull.*, 2013, **38**, 731–736.
13 S.-H. Song, S.-J. Park, T.-J. Bae, K.-M. Jung, W.-H. Park, Y.-S. Kim, Q. F. Yan, S. S. Kim and J.-K. Song, *Nanoscale*, 2020, **12**, 17020–17028.
14 C. Zang, M. Xu, L. Zhang, S. Liu and W. Xie, *J. Mater. Chem. C*, 2021, **9**, 1484–1519.
15 J. Song, O. Wang, H. Shen, Q. Lin, Z. Li, L. Wang, X. Zhang and L. S. Li, *Adv. Funct. Mater.*, 2019, **29**, 1808377.
16 Y. Deng, F. Peng, Y. Lu, X. Zhu, W. Jin, J. Qiu, J. Dong, Y. Hao, D. Di, Y. Gao, T. Sun, M. Zhang, F. Liu, L. Wang, L. Ying, F. Huang and Y. Jin, *Nat. Photonics*, 2022, **16**, 505–511.
17 J. Zhou, M. Zhu, R. Meng, H. Qin and X. Peng, *J. Am. Chem. Soc.*, 2017, **139**, 16556–16567.
18 Y. Yang, Y. Zheng, W. Cao, A. Titov, J. Hyvonen, J. R. Manders, J. Xue, P. H. Holloway and L. Qian, *Nat. Photonics*, 2015, **9**, 259–266.
19 W. Cao, C. Xiang, Y. Yang, Q. Chen, L. Chen, X. Yan and L. Qian, *Nat. Commun.*, 2018, **9**, 2608.
20 Z. Zhang, Y. Ye, C. Pu, Y. Deng, X. Dai, X. Chen, D. Chen, X. Zheng, Y. Gao, W. Fang, X. Peng and Y. Jin, *Adv. Mater.*, 2018, **30**, 1801387.
21 J. Lim, Y.-S. Park, K. Wu, H. J. Yun and V. I. Klimov, *Nano Lett.*, 2018, **18**, 6645–6653.
22 J. Lin, X. Dai, X. Liang, D. Chen, X. Zheng, Y. Li, Y. Deng, H. Du, Y. Ye, D. Chen, C. Lin, L. Ma, Q. Bao, H. Zhang, L. Wang, X. Peng and Y. Jin, *Adv. Funct. Mater.*, 2020, **30**, 1907265.
23 H. Shen, Q. Gao, Y. Zhang, Y. Lin, Q. Lin, Z. Li, L. Chen, Z. Zeng, X. Li, Y. Jia, S. Wang, Z. Du, L. S. Li and Z. Zhang, *Nat. Photonics*, 2019, **13**, 192–197.
24 D. Liu, S. Cao, S. Wang, H. Wang, W. Dai, B. Zou, J. Zhao and Y. Wang, *J. Phys. Chem. Lett.*, 2020, **11**, 3111–3115.
25 C. Pu, X. Dai, Y. Shu, M. Zhu, Y. Deng, Y. Jin and X. Peng, *Nat. Commun.*, 2020, **11**, 937.
26 S. Rhee, J. H. Chang, D. Hahm, B. G. Jeong, J. Kim, H. Lee, J. Lim, E. Hwang, J. Kwak and W. K. Bae, *ACS Nano*, 2020, **14**, 17496–17504.
27 T. Lee, B. J. Kim, H. Lee, D. Hahm, W. K. Bae, J. Lim and J. Kwak, *Adv. Mater.*, 2022, **34**, 2106276.
28 Y. Cheng, Z. Gui, R. Qiao, S. Fang, G. Ba, T. Liang, H. Wan, Z. Zhang, C. Liu, C. Ma, H. Hong, F. Fan, K. Liu and H. Shen, *Adv. Funct. Mater.*, 2022, **32**, 2207974.
29 Z. Li, Y. Hu, H. Shen, Q. Lin, L. Wang, H. Wang, W. Zhao and L. S. Li, *Laser Photonics Rev.*, 2017, **11**, 1600227.
30 Y. Fu, W. Jiang, D. Kim, W. Lee and H. Chae, *ACS Appl. Mater. Interfaces*, 2018, **10**, 17295–17300.
31 X. Li, Q. Lin, J. Song, H. Shen, H. Zhang, L. S. Li, X. Li and Z. Du, *Adv. Opt. Mater.*, 2020, **8**, 1901145.
32 L. Wang, J. Lin, Y. Hu, X. Guo, Y. Lv, Z. Tang, J. Zhao, Y. Fan, N. Zhang, Y. Wang and X. Liu, *ACS Appl. Mater. Interfaces*, 2017, **9**, 38755–38760.
33 T. Kim, K.-H. Kim, S. Kim, S.-M. Choi, H. Jang, H.-K. Seo, H. Lee, D.-Y. Chung and E. Jang, *Nature*, 2020, **586**, 385–389.
34 Z. Yang, Q. Wu, X. Zhou, F. Cao, X. Yang, J. Zhang and W. Li, *Nanoscale*, 2021, **13**, 4562–4568.
35 H. Luo, W. Zhang, M. Li, Y. Yang, M. Guo, S.-W. Tsang and S. Chen, *ACS Nano*, 2019, **13**, 8229–8236.
36 W. Jin, Y. Deng, B. Guo, Y. Lian, B. Zhao, D. Di, X. Sun, K. Wang, S. Chen, Y. Yang, W. Cao, S. Chen, W. Ji, X. Yang, Y. Gao, S. Wang, H. Shen, J. Zhao, L. Qian, F. Li and Y. Jin, *npj Flexible Electron.*, 2022, **6**, 35.
37 E. F. Schubert, LED basics: Optical properties, in *Light-Emitting Diodes*, Cambridge University Press, Cambridge, 2006, pp. 86–100.
38 X. Dai, Y. Deng, X. Peng and Y. Jin, *Adv. Mater.*, 2017, **29**, 1607022.
39 Z. Li, J. Wei, F. Wang, Y. Tang, A. Li, Y. Guo, P. Huang, S. Brovelli, H. Shen and H. Li, *Adv. Energy Mater.*, 2021, **11**, 2101693.
40 D. V. Talapin, J.-S. Lee, M. V. Kovalenko and E. V. Shevchenko, *Chem. Rev.*, 2010, **110**, 389–458.

41 H. Shen, W. Cao, N. T. Shewmon, C. Yang, L. S. Li and J. Xue, *Nano Lett.*, 2015, **15**, 1211–1216.
42 X. Li, Y.-B. Zhao, F. Fan, L. Levina, M. Liu, R. Quintero-Bermudez, X. Gong, L. N. Quan, J. Fan, Z. Yang, S. Hoogland, O. Voznyy, Z.-H. Lu and E. H. Sargent, *Nat. Photonics*, 2018, **12**, 159–164.
43 S. Yang, D. Prendergast and J. B. Neaton, *Nano Lett.*, 2012, **12**, 383–388.
44 P. R. Brown, D. Kim, R. R. Lunt, N. Zhao, M. G. Bawendi, J. C. Grossman and V. Bulović, *ACS Nano*, 2014, **8**, 5863–5872.
45 C.-H. M. Chuang, P. R. Brown, V. Bulović and M. G. Bawendi, *Nat. Mater.*, 2014, **13**, 796–801.
46 P. Reiss, M. Protière and L. Li, *Small*, 2009, **5**, 154–168.
47 J. H. Chang, P. Park, H. Jung, B. G. Jeong, D. Hahm, G. Nagamine, J. Ko, J. Cho, L. A. Padilha, D. C. Lee, C. Lee, K. Char and W. K. Bae, *ACS Nano*, 2018, **12**, 10231–10239.
48 S. Chen, W. Cao, T. Liu, S.-W. Tsang, Y. Yang, X. Yan and L. Qian, *Nat. Commun.*, 2019, **10**, 765.
49 T. Cheng, F. Wang, W. Sun, Z. Wang, J. Zhang, B. You, Y. Li, T. Hayat, A. Alsaed and Z. A. Tan, *Adv. Electron. Mater.*, 2019, **5**, 1800794.
50 T. Cheng, Z. Wang, S. Jin, F. Wang, Y. Bai, H. Feng, B. You, Y. Li, T. Hayat and Z. A. Tan, *Adv. Opt. Mater.*, 2017, **5**, 1700035.
51 H. Jia, F. Wang and Z. A. Tan, *Nanoscale*, 2020, **12**, 13186–13224.
52 F. Wang, Z. Wang, X. Zhu, Y. Bai, Y. Yang, S. Hu, Y. Liu, B. You, J. Wang, Y. Li and Z. A. Tan, *Small*, 2021, **17**, 2007363.
53 F. Wang, W. Sun, P. Liu, Z. Wang, J. Zhang, J. Wei, Y. Li, T. Hayat, A. Alsaedi and Z. A. Tan, *J. Phys. Chem. Lett.*, 2019, **10**, 960–965.
54 R. A. M. Hikmet, D. V. Talapin and H. Weller, *J. Appl. Phys.*, 2003, **93**, 3509–3514.
55 C. Pu and X. Peng, *J. Am. Chem. Soc.*, 2016, **138**, 8134–8142.
56 B. G. Chae, J. H. Lee, S. Park, E. Lee, C. M. Kwak, M. Jafari, Y. K. Jeong, C. G. Park and J. B. Seol, *ACS Nano*, 2018, **12**, 12109–12117.
57 J. Shah, Exciton Dynamics, in *Ultrafast Spectroscopy of Semiconductors and Semiconductor Nanostructures*, Springer Berlin Heidelberg, Berlin, Heidelberg, 1996, pp. 225–261.
58 Y. Cheng, H. Wan, T. Liang, C. Liu, M. Wu, H. Hong, K. Liu and H. Shen, *J. Phys. Chem. Lett.*, 2021, **12**, 5967–5978.
59 K.-H. Lee, J.-H. Lee, W.-S. Song, H. Ko, C. Lee, J.-H. Lee and H. Yang, *ACS Nano*, 2013, **7**, 7295–7302.
60 Y.-S. Park, W. K. Bae, L. A. Padilha, J. M. Pietryga and V. I. Klimov, *Nano Lett.*, 2014, **14**, 396–402.
61 J. Lim, B. G. Jeong, M. Park, J. K. Kim, J. M. Pietryga, Y.-S. Park, V. I. Klimov, C. Lee, D. C. Lee and W. K. Bae, *Adv. Mater.*, 2014, **26**, 8034–8040.
62 B. N. Pal, Y. Ghosh, S. Brovelli, R. Laocharoensuk, V. I. Klimov, J. A. Hollingsworth and H. Htoon, *Nano Lett.*, 2012, **12**, 331–336.
63 Z. Li, F. Chen, L. Wang, H. Shen, L. Guo, Y. Kuang, H. Wang, N. Li and L. S. Li, *Chem. Mater.*, 2018, **30**, 3668–3676.
64 D. Bozyigit, O. Yarema and V. Wood, *Adv. Funct. Mater.*, 2013, **23**, 3024–3029.
65 H. Li, Y. Bian, W. Zhang, Z. Wu, T. K. Ahn, H. Shen and Z. Du, *Adv. Funct. Mater.*, 2022, **32**, 2204529.
66 S. Xie, H. Zhu, M. Li and V. Bulović, *Appl. Phys. Lett.*, 2022, **120**, 211104.
67 D. Bozyigit, V. Wood, Y. Shirasaki and V. Bulovic, *J. Appl. Phys.*, 2012, **111**, 113701.
68 Z. Wu, P. Liu, X. Qu, J. Ma, W. Liu, B. Xu, K. Wang and X. W. Sun, *Adv. Opt. Mater.*, 2021, **9**, 2100389.